Measurement of Dipole Matrix Elements with a Single Trapped Ion

M. Hettrich,[1,*] T. Ruster,[1] H. Kaufmann,[1] C. F. Roos,[2,3] C. T. Schmiegelow,[1]
F. Schmidt-Kaler,[1] and U. G. Poschinger[1]
[1]*QUANTUM, Institut für Physik, Universität Mainz, Staudingerweg 7, 55128 Mainz, Germany*
[2]*Institut für Quantenoptik und Quanteninformation, Österreichische Akademie der Wissenschaften, Technikerstraße 21a, 6020 Innsbruck, Austria*
[3]*Institut für Experimentalphysik, Universität Innsbruck, Technikerstraße 25, 6020 Innsbruck, Austria*
(Received 8 May 2015; published 2 October 2015)

We demonstrate a method to determine dipole matrix elements by comparing measurements of dispersive and absorptive light ion interactions. We measure the matrix element pertaining to the Ca II H line, i.e., the $4^2S_{1/2} \leftrightarrow 4^2P_{1/2}$ transition of $^{40}Ca^+$, for which we find the value 2.8928(43) ea_0. Moreover, the method allows us to deduce the lifetime of the $4^2P_{1/2}$ state to be 6.904(26) ns, which is in agreement with predictions from recent theoretical calculations and resolves a long-standing discrepancy between calculated values and experimental results.

DOI: 10.1103/PhysRevLett.115.143003 PACS numbers: 37.10.Ty, 03.67.Lx, 32.80.Qk

Methods for trapping and cooling single or few atoms, molecules, or ions and manipulating them at the quantum level have opened up new avenues for precision laser spectroscopy. In particular, quantum logic techniques [1] have enabled a new accuracy regime of timekeeping with optical atomic clocks [2]. In contrast to atomic transition frequencies, dipole matrix elements and radiative lifetimes are still notoriously hard to determine at high accuracy, but are important for the quantification of black body radiation shifts of atomic clocks [3], interpretation of astrophysical spectra [4,5], novel approaches for the search for physics beyond standard model [6,7], and for testing the accuracy of atomic structure calculations [8].

Regarding measurements of radiative lifetimes and transition matrix elements, established methods, e.g., based on ion beams, have been successfully complemented by novel techniques based on trapped particles. For ^{87}Rb, dipole matrix elements have been determined on the 10^{-3} uncertainty level by diffraction in a condensate [9], while for the $6p^2P^o_{1/2}$ state of $^{174}Yb^+$, the radiative lifetime has been measured by time-resolved counting of photons emitted from a single trapped ion [10]. A related technique was used for neutral ^{171}Yb in an optical lattice [11].

The species Ca^+ is widely used in quantum optics experiments, and its II H line led to the discovery of the interstellar medium [12]. For $^{40}Ca^+$, branching ratios between different decay channels have been determined at uncertainties approaching the 10^{-5} level [13,14], and lifetimes of metastable states have been accurately measured [15]. The radiative lifetime of the $4^2P_{1/2}$ excited state of $^{40}Ca^+$ has been determined to be 7.098(20) ns [16] by fluorescence measurements on a fast ion beam. However, this value disagrees with the most recent theoretical calculation [8] by more than 11 standard deviations, while similar calculations for alkalinelike species from Li to Fr, Mg^+, Ba^+, and Sr^+ are in good agreement with experimental results (see [8] and references therein).

In this work, we determine the radiative decay rates and the lifetime of the $4^2P_{1/2}$ excited state of $^{40}Ca^+$ together with the dipole matrix element of the $4^2S_{1/2} \leftrightarrow 4^2P_{1/2}$ transition. The cornerstone of our scheme is the comparison between the dispersive and absorptive interactions, which occur upon driving this transition with an off-resonant laser, see Fig. 1. As the method is based on the discrete discrimination of atomic states of a single trapped particle [17,18], it is robust against many systematic error sources which affect other existing methods.

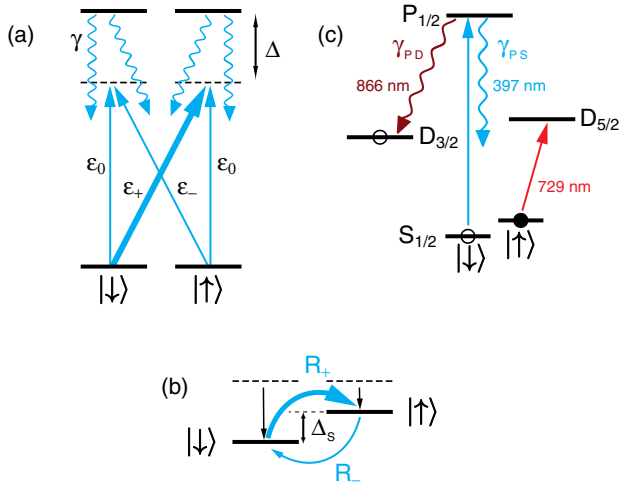

FIG. 1 (color online). Measurement scheme: (a) a laser off-resonantly couples two Zeeman ground state levels to an excited state with decay rate γ. (b) The coupling gives rise to a differential ac-Stark shift Δ_S between the Zeeman levels and incoherent redistribution of population at rates $R_\pm$. (c) Relevant energy levels in $^{40}Ca^+$. The shelving to the metastable $3^2D_{5/2}$ state as well to the $3^2D_{3/2}$ state acting as a population sink are indicated. State populations, which result in a bright (dark) detection event are marked by an open (closed) circle.

The off-resonant laser is characterized by its detuning Δ from the $4^2S_{1/2} \leftrightarrow 4^2P_{1/2}$ transition, the Rabi frequency Ω, and the relative amplitudes ϵ_q, which characterize the circular ($q = \pm 1$, denoted "$\pm$" henceforth) and π ($q = 0$) polarization components.

The *dispersive* interaction with the laser field, detuned by a frequency Δ from resonance, causes ac-Stark shifts [19,20] of the energy levels. Specifically, we are interested in the differential ac-Stark shift Δ_S between the two Zeeman sublevels of the electronic ground state $|S_{1/2}, m_S = \pm 1/2\rangle$, denoted henceforth as $|\uparrow\rangle$ and $|\downarrow\rangle$. It reads

$$\Delta_S = \frac{1}{3}\frac{\Omega^2}{4\Delta}(\epsilon_-^2 - \epsilon_+^2), \tag{1}$$

and is obtained by a spin-echo measurement technique [21].

The *absorptive* interaction mediated by the same laser field manifests itself through inelastic Raman scattering, i.e., spin flips [22,23]. We denote the spin-flip rate from $|\downarrow\rangle$ to $|\uparrow\rangle$ with R_+ and the rate in the inverse direction, respectively, with R_-. For an optical field with arbitrary polarization they read [20]

$$R_\pm = \gamma_{PS}\frac{\epsilon_\pm^2 + \epsilon_0^2}{9}\frac{\Omega^2}{4\Delta^2}, \tag{2}$$

where γ_{PS} is the radiative decay rate from the $P_{1/2}$ to the $S_{1/2}$ state. The spin-flip rates $R_\pm$ are experimentally determined by monitoring the population in $|\uparrow\rangle$ and $|\downarrow\rangle$ during the interaction. Note that the π-polarized field component drives the two spin-flip directions equally strong, whereas each of the circular components drives only one pathway, corresponding to optical pumping in the limit of purely circularly polarized field component. The occurrence of elastic (Rayleigh) scattering is taken into account by the prefactor. The detuning Δ is chosen such that the conditions $|\Delta| \gg \Omega, \gamma_{PS}$ for Eqs. (1) and (2) to hold are met.

By combining Eqs. (1) and (2), we obtain the decay rate γ_{PS}:

$$\gamma_{PS} = 3\Delta\frac{\delta R}{\Delta_S}, \tag{3}$$

with $\delta R = R_- - R_+$. All quantities on the rhs of (3) are experimentally accessible.

As both interactions are driven with the same optical field, the Rabi frequency Ω and the polarization amplitudes ϵ_q cancel out in Eq. (3) and notorious error sources are eliminated. These quantities are given by the electric field amplitude of the off-resonant laser at the position of the ion, which reads $\mathbf{E} = \sum_{q=\pm,1}|\mathbf{E}|\epsilon_q \mathbf{e}_q + \text{c.c.}$ Here, $\mathbf{e}_q$ are the spherical basis vectors. The polarization amplitude ϵ_q defines the coupling between Zeeman sublevels with $m_P - m_S = q$ with effective Rabi frequencies scaled with the respective Wigner $3j$ symbol,

$$\Omega\epsilon_q \begin{pmatrix} 1/2 & 1 & 1/2 \\ -m_S & q & m_P \end{pmatrix}.$$

Here $\Omega = 2|\mathbf{E}|\mathcal{D}/\hbar$ is defined as the base Rabi frequency, with the reduced dipole matrix element $\mathcal{D} = \langle S_{1/2}\|\hat{\mathbf{d}}\|P_{1/2}\rangle$.

We take an additional decay channel into account, for the case of $^{40}Ca^+$ decay from the $4^2P_{1/2}$ to the $3^2D_{3/2}$ state occurs at rate γ_{PD}. For that, we assume that only circular components are present in the beam, i.e., $\epsilon_0^2 \approx 0$. The rates at which population from $|\uparrow\rangle(|\downarrow\rangle)$ is sunk in the metastable $3^2D_{3/2}$ state are then proportional to $R_\pm$:

$$R_{\uparrow(\downarrow)D} = 3(\gamma_{PD}/\gamma_{PS})R_{-(+)} \equiv bR_{-(+)}, \tag{4}$$

with the leak factor b, which is also accessible from the measured time-dependent populations. Together with γ_{PD}, we obtain also the $4^2P_{1/2}$ state's lifetime τ. Finally, using γ_{PS} and the resonance wavelength λ_{PS} of the $4^2S_{1/2} \leftrightarrow 4^2P_{1/2}$ transition, we can deduce the reduced matrix element $\mathcal{D}$:

$$\mathcal{D}^2 = 2\gamma_{PS}\frac{3\epsilon_0\hbar}{8\pi^2}\lambda_{PS}^3. \tag{5}$$

We perform measurements on a single $^{40}Ca^+$ ion stored in a segmented Paul trap [24]. The relevant energy levels and transitions are depicted in Fig. 1. A magnetic field splits the Zeeman sublevels of the electronic ground state $|\uparrow\rangle$ and $|\downarrow\rangle$ by $2\pi \times 13.7$ MHz. The ion is Doppler cooled on the $4^2S_{1/2} \leftrightarrow 4^2P_{1/2}$ (cycling) transition near 397 nm and afterwards prepared in either $|\uparrow\rangle$ or $|\downarrow\rangle$ by optical pumping. Now, the ion is illuminated with light near 397 nm, detuned by Δ from the $4^2S_{1/2} \leftrightarrow 4^2P_{1/2}$ transition to induce both the dispersive and absorptive interactions, which allow for determining Δ_S and $R_\pm$. Spin readout is accomplished by shelving population from the $|\uparrow\rangle$ level to the metastable $3^2D_{5/2}$ state by means of rapid adiabatic passage pulses [18,25]. This allows for discrimination between $|\uparrow\rangle$ and $|\downarrow\rangle$ as the linewidth of the $4^2S_{1/2} \leftrightarrow 3^2D_{5/2}$ quadrupole transition and the bandwidth of the rapid adiabatic passage pulses are much smaller than the Zeeman splitting. Then, the ion is illuminated by laser fields driving the cycling transition and the $3^2D_{3/2} \leftrightarrow 4^2P_{1/2}$ transition near 866 nm, such that fluorescence is detected on a photomultiplier tube if the ion has not been shelved. Conversely, the probability to not detect fluorescence, i.e., for a dark event, corresponds to the probability that the ion has been shelved from $|\uparrow\rangle$ to the metastable state.

The off-resonant laser light is provided by an amplified and frequency-doubled diode laser system, stabilized in both wavelength ($\delta\Delta/\Delta \lesssim 0.5 \times 10^{-3}$) and intensity ($\delta I/I \lesssim 0.5 \times 10^{-3}$). The beam is aligned along the quantizing magnetic field and predominantly σ^+ polarized, such that $R_+ \gg R_-$, and $\epsilon_0^2 \approx 0$, justifying the approximation for Eq. (4).

The ac-Stark shift Δ_S is measured with a spin-echo sequence, where a $\pi/2$ pulse on the stimulated Raman transition between $|\uparrow\rangle$ and $|\downarrow\rangle$ is followed by a π pulse, and another $\pi/2$ pulse concludes the sequence. The delay time between the pulses is constant. During the first delay, the

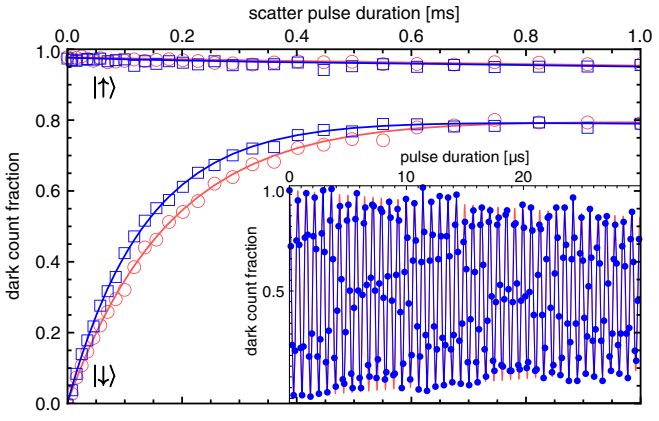

FIG. 2 (color online). Dark event fraction versus time of exposure to an off-resonant laser pulse for initializations in $|\uparrow\rangle$ and $|\downarrow\rangle$. Data points indicated by blue squares (red circles) are measured with the laser detuned by 12.03 GHz (13.94 GHz) from resonance. Solid lines show the fits to the model, Eq. (7). The inset shows the dark event fraction versus pulse duration for a spin-echo experiment. The blue line connects the data points, the red line is the resulting fit. The oscillation frequency directly corresponds to the differential ac-Stark shift Δ_S.

ion is exposed to a square pulse of variable duration from the off-resonant laser. We probe 250 different shift pulse times, each with 150 interrogations. The pulse durations are spaced by 120 ns, such that a signal with about 40 oscillation periods is obtained. The differential ac-Stark shift is the frequency of this oscillatory dark event fraction (see inset of Fig. 2).

For the measurement of the spin-flip rates $R_{\pm}$, the ion is exposed to pulses of variable duration up to 1 ms of the off-resonant laser after preparation. This changes the spin populations as depicted in Fig. 2. The time gap between initialization and readout is kept constant irrespectively of the scatter pulse duration to avoid systematic effects.

The spin-flip dynamics can be described by the rate equations

$$\dot{p}_{\uparrow} = -R_{-}(1+b)p_{\uparrow} + R_{+}p_{\downarrow},$$
$$\dot{p}_{\downarrow} = -R_{+}(1+b)p_{\downarrow} + R_{-}p_{\uparrow}. \quad (6)$$

The solution of Eqs. (6) is

$$p_{\uparrow}^{(\uparrow)}(t) = \frac{1}{\tilde{R}} e^{-(1/2)\bar{R}t}\left[\tilde{R}\cosh\left(\frac{\tilde{R}t}{2}\right) - (1+b)\delta R \sinh\left(\frac{\tilde{R}t}{2}\right)\right],$$
$$p_{\uparrow}^{(\downarrow)}(t) = \frac{2}{\tilde{R}} e^{-(1/2)\bar{R}t} R_{+}\sinh(\tilde{R}t/2), \quad (7)$$

with $p_{\uparrow}^{(\uparrow)}$ corresponding to initialization in $|\uparrow\rangle$, $p_{\uparrow}(t=0)=1$, and $p_{\uparrow}^{(\downarrow)}$ for initialization in $|\downarrow\rangle$, $p_{\downarrow}(t=0)=1$. We use $\bar{R} = (1+b)(R_{-}+R_{+})$ and $\tilde{R}^2 = \bar{R}^2 - 4b(2+b)R_{-}R_{+}$.

For each measurement, the dark event fraction is determined by probing the ion 2500 times for 30 fixed scatter pulse durations. Note that while the ac-Stark shift is given by the frequency of an oscillatory signal, the spin-flip rates are given by time constants of exponentially decaying signals. Thus, the latter measurement requires significantly more data to attain the same level of precision as the former. We extract the values for the differential scattering rate δR and the leak factor b by means of a Markov chain Monte Carlo parameter estimation, taking into account the binomial statistics of the shot noise in the spin readout. State preparation and measurement errors are taken into account by modeling the measured dark event fractions as a linear transformation of the values $p_{\uparrow}^{(\uparrow)}(t)$, $p_{\uparrow}^{(\downarrow)}(t)$ from Eqs. (7).

We repeated ac-Stark shift measurements and spin-flip rate measurements in an interleaved fashion in order to capture drifts of the laser intensity and thus the Rabi frequency Ω. One measurement run consists of one spin-flip rate measurement for preparation both in $|\uparrow\rangle$ and $|\downarrow\rangle$, preceded and followed by one ac-Stark shift measurement. In total, 65 of such measurement runs were performed, at a total acquisition time of about 50 h. Four different values of the detuning Δ were used to show that no systematic effects with respect to this parameter are present. To determine the value of these detunings, we read the optical frequency from a commercial wavelength meter (High Finesse WSU 267) with better than 10 MHz precision. We perform a linear regression of the measured Δ_S divided by δR versus the corresponding optical frequencies to obtain the resonance frequency, as shown in Fig. 3. Compared to direct fluorescence spectroscopy, this technique mitigates effects like

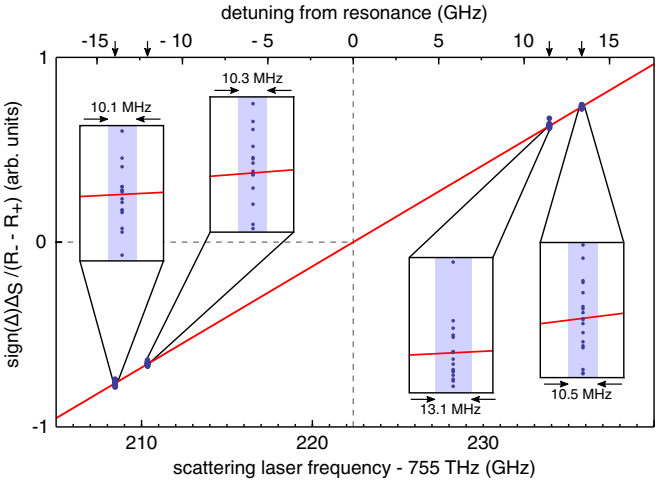

FIG. 3 (color online). Determination of the four detunings chosen for our measurements. For each of the 65 acquired data sets, we plot the quantity $\mathrm{sign}(\Delta)\Delta_S/\delta R \propto \Delta$ versus the optical frequency as measured by a wavelength meter. The zero crossing of a linear fit, depicted by the solid red line, reveals the resonance frequency with a standard measurement uncertainty of $2\pi \times 21$ MHz. The insets show details of the data sets measured at the different detunings with the abscissa magnified 166 times. The shaded backgrounds indicate their uncertainties along the frequency axis. The arrows on the top frequency scale indicate the values of the four different detunings at -13.94, -12.03, 11.52, and 13.42 GHz.

TABLE I. List of relative corrections and measurement uncertainties for γ_{PS}. The specified values result from averaging over the 65 sets of measurement data. They are added in quadrature to obtain the resulting final uncertainty.

Effect	Shift$\times 10^{-3}$	Uncertainty$\times 10^{-3}$
Residual ϵ_0 polarized light	3.3	2.9
Uncertainty of resonance frequency	…	1.6
Statistical uncertainty of δR	…	1.5
Residual near-resonant light	−0.4	0.5
Wave-meter precision	…	0.4
$D_{3/2}$ depletion	0.3	0.2
Uncertainty of Δ_S	…	0.2
Influence of micromotion	…	0.1
Influence of $P_{3/2}$ state	0.3	<0.1
Residual line-broadening effects	0.1	<0.1
Total	+3.6	3.7

power broadening, Zeeman splitting, or micromotion induced broadening, which would make a determination of the resonance frequency less accurate.

Finally, we combine the measured quantities Δ, Δ_S, and δR, using Eq. (3), to obtain the desired value γ_{PS}. Together with b this also yields $\gamma_{PD} = (b/3)\gamma_{PS}$, and the radiative lifetime is given by $1/\tau = \gamma_{PS}[1 + (b/3)]$.

Averaging over the data sets and taking into account the corrections discussed below, we obtain the resulting values: $\gamma_{PS} = 2\pi \times 21.57(8)$ MHz and a $4^2P_{1/2} \to 4^2S_{1/2}$ branching fraction of $1/[1 + (b/3)] = 0.935\,72(25)$. This leads to a lifetime of $\tau = 6.904(26)$ ns and a value of $\gamma_{PD} = 2\pi \times 1.482(8)$ MHz. Using Eq. (5), we obtain a value for the reduced dipole matrix element of $\mathcal{D} = 2.8928(43)\ ea_0$.

Experimental imperfections and model approximations lead to uncertainties and corrections for the value of γ_{PS}. These are summarized in Table I: Beyond the approximation in Eq. (4), a possible ϵ_0 polarization component has been taken into account, and yields corrections and uncertainties on the 10^{-3} level. The uncertainty of the detuning Δ is determined by the finite precision of the wavelength meter, and by the uncertainty of the determination of the resonance frequency, see Fig. 3. The random measurement errors for δR, determined by the amount of acquired data, are another significant contribution to the uncertainty budget. Residual resonant light close to 397 nm resulting from imperfect laser switch off causes relative corrections and uncertainties in the 10^{-4} regime. Beyond the rate equation model Eq. (6), we include a correction for the finite lifetime of the $3^2D_{3/2}$ state or its depletion by residual light near 866 nm. Δ_S can be measured by orders of magnitude more precisely than δR and b; however, the precision is limited by drift effects, quantified by monitoring the ac-Stark shift over the entire data acquisition time. Excess micromotion of the ion also causes a small systematic uncertainty via frequency modulation of the off-resonant light. Furthermore, we include corrections due to the

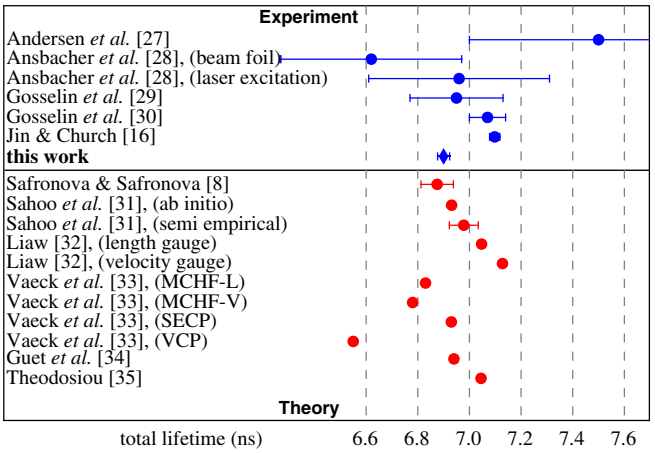

FIG. 4 (color online). Comparison of the measured lifetime with theoretical and experimental results for $P_{1/2}$-level lifetimes from Refs. [8,16,27–35].

presence of the $4^2P_{3/2}$ state about $2\pi \times 6.69$ THz above the $4^2P_{1/2}$ state, and due to the power-broadened Lorentzian line shape beyond the assumption $|\Delta| \gg \Omega, \gamma_{PS}$. A detailed discussion of corrections and uncertainties is presented in the Supplemental Material [26].

Our value for τ is compared to previously reported values in Fig. 4. We find that our value agrees with the latest theory predictions [8], while it is in substantial disagreement with the most recent experimental result [16]. Our value for the branching fraction is in agreement with the results from recent measurements [14]. To our knowledge, there is no experimentally determined value of $\mathcal{D}$ so far. The value reported in our work is in agreement with the calculation from [8].

Furthermore, using the measured value for $\mathcal{D}$, we infer the reduced matrix element pertaining to the $4^2S_{1/2} \leftrightarrow 4^2P_{3/2}$ transition, which results to $\langle S_{1/2}\|\hat{\mathbf{d}}\|P_{3/2}\rangle = \sqrt{2}\mathcal{D} = 4.091(6)\ ea_0$. Both reduced dipole matrix elements enter in the calculation of the blackbody-radiation (BBR) shift of the $4^2S_{1/2} \leftrightarrow 3^2D_{3/2}$ and $4^2S_{1/2} \leftrightarrow 3^2D_{5/2}$ quadrupole transitions, which are widely used test beds for high precision laser spectroscopy [36]. The BBR shift is among the major contributions to the uncertainties of clock transition frequencies, for species such as $^{43}Ca^+$ [37], Sr^+ [38], Sr [39,40], and Yb [41]. These are used for state-of-the art optical clock experiments, and some of them are discussed as new Systeme International frequency standards. Our result adds to existing work [42–44] validating computational methods used to predict the BBR shift in optical clocks.

In summary, we demonstrate a novel method for the measurement of dipole matrix elements, which works despite the presence of additional decay channels. We attain an uncertainty on the 10^{-3} level. All major error sources can be potentially mitigated, such that measurements of radiative decay rates at unprecedentedly low uncertainties in the 10^{-4} regime appear within reach with current technology. Our method is applicable to atom and ion species which allow for the preparation and readout of Zeeman or hyperfine sublevels.

We acknowledge financial support by the European commission within the IP SIQS and by the Bundesministerium für Bildung und Forschung via IKT 2020 (Q.com). U. G. P. acknowledges funding by the Johannes-Gutenberg Universität Mainz via internal university research funding grant "Trapped ions in phase-stabilized standing waves." C. T. S. acknowledges support from the BMBF via the Alexander von Humboldt Foundation. We thank Vladan Vuletic, Rene Gerritsma, and Marianna Safronova for helpful discussions.

*hettrich@uni-mainz.de
http://www.quantenbit.de

[1] P. O. Schmidt, T. Rosenband, C. Langer, W. M. Itano, J. C. Bergquist, and D. J. Wineland, Science **309**, 749 (2005).
[2] T. Rosenband, D. B. Hume, P. O. Schmidt, C. W. Chou, A. Brusch, L. Lorini, W. H. Oskay, R. E. Drullinger, T. M. Fortier, J. E. Stalnaker, S. A. Diddams, W. C. Swann, N. R. Newbury, W. M. Itano, D. J. Wineland, and J. C. Bergquist, Science **319**, 1808 (2008).
[3] M. S. Safronova, M. G. Kozlov, and C. W. Clark, Phys. Rev. Lett. **107**, 143006 (2011).
[4] E. Rauscher and G. W. Marcy, Publ. Astron. Soc. Pac. **118**, 617 (2006).
[5] M. Carlsson and J. Leenaarts, Astron. Astrophys. **539**, A39 (2012).
[6] N. Fortson, Phys. Rev. Lett. **70**, 2383 (1993).
[7] T. W. Koerber, M. H. Schacht, K. R. G. Hendrickson, W. Nagourney, and E. N. Fortson, Phys. Rev. Lett. **88**, 143002 (2002).
[8] M. S. Safronova and U. I. Safronova, Phys. Rev. A **83**, 012503 (2011).
[9] C. D. Herold, V. D. Vaidya, X. Li, S. L. Rolston, J. V. Porto, and M. S. Safronova, Phys. Rev. Lett. **109**, 243003 (2012).
[10] S. Olmschenk, D. Hayes, D. N. Matsukevich, P. Maunz, D. L. Moehring, K. C. Younge, and C. Monroe, Phys. Rev. A **80**, 022502 (2009).
[11] K. Beloy, J. A. Sherman, N. D. Lemke, N. Hinkley, C. W. Oates, and A. D. Ludlow, Phys. Rev. A **86**, 051404 (2012).
[12] J. Hartmann, Astrophys. J. **19**, 268 (1904).
[13] R. Gerritsma, G. Kirchmair, F. Zähringer, J. Benhelm, R. Blatt, and C. F. Roos, Eur. Phys. J. D **50**, 13 (2008).
[14] M. Ramm, T. Pruttivarasin, M. Kokish, I. Talukdar, and H. Häffner, Phys. Rev. Lett. **111**, 023004 (2013).
[15] A. Kreuter, C. Becher, G. P. T. Lancaster, A. B. Mundt, C. Russo, H. Häffner, C. Roos, W. Hänsel, F. Schmidt-Kaler, R. Blatt, and M. S. Safronova, Phys. Rev. A **71**, 032504 (2005).
[16] J. Jin and D. A. Church, Phys. Rev. Lett. **70**, 3213 (1993).
[17] D. Leibfried, R. Blatt, C. Monroe, and D. Wineland, Rev. Mod. Phys. **75**, 281 (2003).
[18] U. G. Poschinger, G. Huber, F. Ziesel, M. Deiss, M. Hettrich, S. A. Schulz, G. Poulsen, M. Drewsen, R. J. Hendricks, K. Singer, and F. Schmidt-Kaler, J. Phys. B **42**, 154013 (2009).
[19] R. Grimm and M. Weidemüller, Adv. At. Mol. Opt. Phys. **42**, 95 (2000).
[20] D. J. Wineland, M. Barret, J. Britton, J. Chiaverini, B. DeMarco, W. M. Itano, B. Jelenkovic, C. Langer, D. Leibfried, V. Meyer, T. Rosenband, and T. Schätz, Phil. Trans. R. Soc. A **361**, 1349 (2003).
[21] H. Häffner, S. Gulde, M. Riebe, G. Lancaster, C. Becher, J. Eschner, F. Schmidt-Kaler, and R. Blatt, Phys. Rev. Lett. **90**, 143602 (2003).
[22] R. Ozeri, C. Langer, J. D. Jost, B. DeMarco, A. Ben-Kish, B. R. Blakestad, J. Britton, J. Chiaverini, W. M. Itano, D. B. Hume, D. Leibfried, T. Rosenband, P. O. Schmidt, and D. J. Wineland, Phys. Rev. Lett. **95**, 030403 (2005).
[23] H. Uys, M. J. Biercuk, A. P. VanDevender, C. Ospelkaus, D. Meiser, R. Ozeri, and J. J. Bollinger, Phys. Rev. Lett. **105**, 200401 (2010).
[24] S. Schulz, U. Poschinger, F. Ziesel, and F. Schmidt-Kaler, New J. Phys. **10**, 045007 (2008).
[25] C. Wunderlich, T. K. Th. Hannemann and, H. Häffner, C. Roos, W. Hänsel, R. Blatt, and F. Schmidt-Kaler, J. Mod. Opt. **54**, 1541 (2007).
[26] See Supplemental Material at http://link.aps.org/supplemental/10.1103/PhysRevLett.115.143003 for a detailed error discussion.
[27] T. Andersen, J. Desesquelles, K. A. Jessen, and G. Sørensen, J. Quant. Spectrosc. Radiat. Transfer **10**, 1143 (1970).
[28] W. Ansbacher, A. S. Inamdar, and E. H. Pinnington, Phys. Lett. **110A**, 383 (1985).
[29] R. N. Gosselin, E. H. Pinnington, and W. Ansbacher, Nucl. Instrum. Methods Phys. Res., Sect. B **31**, 305 (1988).
[30] R. N. Gosselin, E. H. Pinnington, and W. Ansbacher, Phys. Rev. A **38**, 4887 (1988).
[31] B. K. Sahoo, B. P. Das, and D. Mukherjee, Phys. Rev. A **79**, 052511 (2009).
[32] S.-S. Liaw, Phys. Rev. A **51**, R1723 (1995).
[33] N. Vaeck, M. Godefroid, and C. Froese Fischer, Phys. Rev. A **46**, 3704 (1992).
[34] C. Guet and W. R. Johnson, Phys. Rev. A **44**, 1531 (1991).
[35] C. E. Theodosiou, Phys. Rev. A **39**, 4880 (1989).
[36] M. Chwalla, J. Benhelm, K. Kim, G. Kirchmair, T. Monz, M. Riebe, P. Schindler, A. S. Villar, W. Hänsel, C. F. Roos, R. Blatt, M. Abgrall, G. Santarelli, G. D. Rovera, and P. Laurent, Phys. Rev. Lett. **102**, 023002 (2009).
[37] B. Arora, M. S. Safronova, and C. W. Clark, Phys. Rev. A **76**, 064501 (2007).
[38] P. Dubé, A. A. Madej, Z. Zhou, and J. E. Bernard, Phys. Rev. A **87**, 023806 (2013).
[39] M. S. Safronova, S. G. Porsev, U. I. Safronova, M. G. Kozlov, and C. W. Clark, Phys. Rev. A **87**, 012509 (2013).
[40] B. J. Bloom, T. L. Nicholson, J. R. Williams, S. L. Campbell, M. Bishof, X. Zhang, W. Zhang, S. L. Bromley, and J. Ye, Nature (London) **506**, 71 (2014).
[41] A. D. Ludlow, M. M. Boyd, J. Ye, E. Peik, and P. O. Schmidt, Rev. Mod. Phys. **87**, 637 (2015).
[42] K. Beloy, N. Hinkley, N. B. Phillips, J. A. Sherman, M. Schioppo, J. Lehman, A. Feldman, L. M. Hanssen, C. W. Oates, and A. D. Ludlow, Phys. Rev. Lett. **113**, 260801 (2014).
[43] P. Dubé, A. A. Madej, M. Tibbo, and J. E. Bernard, Phys. Rev. Lett. **112**, 173002 (2014).
[44] T. Middelmann, S. Falke, C. Lisdat, and U. Sterr, Phys. Rev. Lett. **109**, 263004 (2012).